Neuro-Oncology 12(12):1231–1243, 2010.
doi:10.1093/neuonc/noq101
Advance Access publication August 17, 2010

Targeting Notch pathway induces growth inhibition and differentiation of neuroblastoma cells

Giulia Ferrari-Toninelli, Sara Anna Bonini, Daniela Uberti, Laura Buizza, Paola Bettinsoli, Pietro Luigi Poliani, Fabio Facchetti, and Maurizio Memo

Department of Biomedical Sciences and Biotechnologies, University of Brescia Medical School and National Institute of Neuroscience (G.F.-T., S.A.B., D.U., L.B., P.B., M.M.), Department of Pathology (P.L.P., F.F.), University of Brescia Medical School, Brescia, Italy

High-risk neuroblastoma is a severe pediatric tumor characterized by poor prognosis. Understanding the molecular mechanisms involved in tumor development and progression is strategic for the improvement of pharmacological therapies. Notch was recently proposed as a pharmacological target for the therapy of several cancers and is emerging as a new neuroblastoma-related molecular pathway. However, the precise role played by Notch in this cancer remains to be studied extensively. Here, we show that Notch activation by the Jagged1 ligand enhances the proliferation of neuroblastoma cells, and we propose the possible use of Notch-blocking γ-secretase inhibitors (GSIs) in neuroblastoma therapy. Two different GSIs, Compound E and DAPT, were tested alone or in combination with 13-*cis* retinoic acid (RA) on neuroblastoma cell lines. SH-SY5Y and IMR-32 cells were chosen as paradigms of lower and higher malignancy, respectively. Used alone, GSIs induced complete cell growth arrest, promoted neuronal differentiation, and significantly reduced cell motility. The combination of GSIs and 13-*cis* RA resulted in the enhanced growth inhibition, differentiation, and migration of neuroblastoma cells. In summary, our data suggest that a combination of GSIs with 13-*cis* RA offers a therapeutic advantage over a single agent, indicating a potential novel therapy for neuroblastoma.

Keywords: γ-secretase inhibitors, 13-*cis* retinoic acid, cell migration, differentiation, neuroblastoma.

Neuroblastoma represents the most common extracranial solid cancer in childhood and accounts for 6%–10% of pediatric tumors. About half of all children with neuroblastoma are classified as high-risk patients and, despite intensive therapeutic regimens, in these patients survival is less than 40%.[1] An improvement in the high-risk neuroblastoma outcome should be obtained by the complete eradication of the "minimal residual disease," which is responsible for the high degree of relapses that impair long-term survival.[2] At present, minimal residual disease is prevented by repeated courses of the 13-*cis* retinoic acid (RA) treatment;[3] however, this treatment resulted in a modest improvement of the patients' outcome mainly due to acquired resistance mechanisms. Recently, retinoids have been shown to interact with several other pathways; so multiple therapies using retinoids in combination with other pharmacological agents are now the subjects of studies.[4] Some compounds, including histone deacetylase inhibitors and interferons, are at present in clinical trials;[5,6] however, new molecules are continuously screened.[7] New knowledge about the molecular mechanisms that regulate neuroblastoma development and progression is then needed to design innovative therapeutic approaches and to improve the existing therapies.[8,9]

Notch is the emerging as a new signaling pathway in neuroblastoma. Notch pathway is part of a receptor family (Notch1–4) activated by ligands (Jagged and Delta) present on neighboring cells. Upon ligand binding, Notch receptors are cleaved by the γ-secretase complex, resulting in the release of an active intracellular domain (NICD, Notch intracellular domain), that translocates to the nucleus and modulates gene expression.[10]

In normal tissues, Notch regulates the cell-lineage decisions during embryogenesis[11] and modulates the differentiated state in mature cells.[12–14] Considerable

Received September 18, 2009; accepted July 7, 2010.

Corresponding Author: Giulia Ferrari-Toninelli, MD, PhD, Department of Biomedical Sciences and Biotechnologies and National Institute of Neuroscience, University of Brescia Medical School, Viale Europa 11, 25123 Brescia, Italy (giuliaferraritoninelli@yahoo.it).

evidence suggest that Notch signaling plays a critical role also in the progression of several cancers through the regulation of the main cellular functions associated with tumorigenesis, such as proliferation, angiogenesis, and cell migration.[15–18]

The Notch pathway is also considered one of the main factors in the regulation of "cancer stem cells."[19] γ-secretase inhibitors (GSIs), which block Notch receptor cleavage and the consequent Notch pathway activation, were successfully proposed as a cancer therapy.[20,21] GSIs were shown to inhibit cell proliferation and induce cell differentiation in several cancer models, both in vitro and in vivo,[22–24] and clinical trials are now in progress for some of these compounds.[25]

Some observations suggest Notch as one of the pathways involved in neuroblastoma pathogenesis, particularly related to its key role in the neural embryonic development.[26] In fact, it is believed that neuroblastoma originates from precursor cells of the sympathetic nervous system that failed to complete their normal differentiation program and was recently found that the Notch pathway inhibits neuronal differentiation and maintains sympathetic precursors in a proliferative state.[27] Furthermore, the Notch pathway is activated by the homeobox transcription factor PHOX2B, an important regulator of peripheral sympathetic nervous system differentiation that was found to be mutated in some cases of familial and sporadic neuroblastoma.[28]

In neuroblastoma cell lines, several data indicate that Notch signaling prevents neuronal differentiation; in fact, neuroblastoma cell differentiation is inhibited by Notch1,[29] and Notch overexpressing neuroblastoma cells are resistant to RA differentiation;[30] furthermore, the Notch effector Hes1 was found to be induced by TGF-α in human neuroblastoma cells, resulting in the maintenance of neoplastic transformation.[31]

Under hypoxic conditions that induce dedifferentiation of neuroblastoma cells, the Notch pathway is activated, leading to more aggressive phenotype stem cell–like characteristics.[32]

A relation between the Notch pathway and the *MYCN* gene was also found. *MYCN* gene amplification is related to the high aggressiveness and poor prognosis of the cancer.[33] The overexpression of N-Myc in mouse fibroblasts induced an increase in the Notch ligand DLL3 and the activation of Notch1 receptor.[34] In an *MYCN*-amplified neuroblastoma cell line, N-Myc downregulation was found to decrease the Notch1 levels and induce neuronal differentiation.[35]

Finally, a Notch signaling antagonist was shown to inhibit tumor growth and angiogenesis in a neuroblastoma mouse model, suggesting Notch blocking as a potential therapy.[36]

The present study is aimed to validate in vitro the use of GSIs for the treatment of neuroblastoma.

A correlation between Notch pathway activation and neuroblastoma cell proliferation was first demonstrated. Then, the GSI efficacy was evaluated by the analysis of the proliferation rate, morphological differentiation, and migration capability of 2 neuroblastoma cell lines, SH-SY5Y and IMR-32, representative of 2 different malignancy degrees.

GSIs were tested either as single agents or in association with 13-*cis* RA to verify the possible therapeutic advantage offered by the combination of these agents.

Materials and Methods

Cell Lines

The human SH-SY5Y neuroblastoma cell line (DSMZ) was cultured in a 1:1 mixture of Ham's F12 nutrient and Dulbecco's modified Eagle's medium (Sigma-Aldrich) supplemented with 10% fetal bovine serum (FBS, Sigma-Aldrich), 2 mM L-glutamine, 50 μg/mL penicillin, and 100 μg/mL streptomycin (Sigma-Aldrich). The IMR-32 neuroblastoma cell line (DSMZ) and the KELLY neuroblastoma cell line (Sigma-Aldrich) were grown in the RPMI medium (Sigma-Aldrich) supplemented with 10% FBS (Sigma-Aldrich), 2 mM L-glutamine, 50 μg/mL penicillin, 100 μg/mL streptomycin (Sigma-Aldrich), and 1× MEM nonessential amino acid solution (Sigma-Aldrich). SH-SY5Y cells stably transfected with amyloid precursor protein (APP) 751 wild type (SH-SY5Y-APPwt) were cultured in a complete SH-SY5Y cell medium with geneticin sulfate antibiotic (G418, Invitrogen) at a final concentration of 300 μg/mL. All the cell lines were grown at 37°C in a 95% air–5% CO_2 humidified incubator.

Drug Treatments

Jagged1 (CDDYYYGFGCNKFCRPR, corresponding to Jagged1 residues 188–204) and the scramble peptide (RCGPDCFDNYGRYKYCF) were synthesized according to Nickoloff et al.[37] (Primm srl, San Raffaele Biomedical Science Park) and added to the culture medium at the concentration of 40 μM and for different times, as indicated.

GSIs IX (DAPT) and XXI (compound E [CpdE]; CalBiochem, EMD Biosciences) were added to the culture medium at 10 μM for different times, as indicated. 13-*cis* RA (Sigma-Aldrich) was added to the culture medium at 1 μM, for different times, as indicated. GSI XI (JLK6; CalBiochem, EMD Biosciences) was added to the culture medium at 1 μM for 5 days.

Proliferation and Cell Viability

Cell number and viability were determined by the Trypan blue exclusion test. For proliferation, cells were treated for 24–48 hours with 40 μM Jagged1 peptide, and then fixed with 4% PFA and immunostained with an anti-Ki-67 antibody (Ki-67 clone MIB-1, Dako; 1:100) and with the appropriate secondary antibody (Dako). The antigens were visualized by reaction with 3,30-diaminobenzidine tetrahydrochloride (0.05%; DAB, Sigma-Aldrich) as a chromogen and hydrogen peroxide (0.003%), and cells were counterstained with

hematoxylin. Images were taken through an Olympus phase contrast microscope (×20 magnification); Ki-67 positive nuclei were determined by counting at least 10 fields for each treatment.

Flow Cytometry for Analysis of Cell Cycle and Apoptosis

For cell cycle analysis, cells were harvested at the completion of the respective treatments and washed with phosphate-buffered saline (PBS; pH 7.4) twice before being fixed with 70% ethyl alcohol for 15 minutes at −20°C. Subsequently, the cells were centrifuged at 450 g for 5 minutes. Before flow cytometric analysis, cells were resuspended in 200 μL of 20 μg/mL propidium iodide (PI; Bender Medsystems) for staining cellular DNA. The cellular DNA content was then analyzed using a Partec Space Flow Cytometer (Partec).

For the apoptosis analysis, after treatment, cells were washed with PBS and stained with Annexin V-FITC and PI using the Apoptosis Detection Kit (Bender Medsystems) according to the manufacturer's protocol. Annexin-positive cells were counted using a Partec Space Flow Cytometer (Partec) within 1 hour after staining. Data analysis was carried out using FlowJo software (Tree star).

Immunofluorescence and Morphometric Analysis

SH-SY5Y cells were plated with a density of 75×10^3 per well in a 24-well plate, grown on a glass coverslip coated with poly-L-lysine (Sigma-Aldrich); IMR-32 cells were plated with a density of 50×10^3 per well and grown on a glass coverslip coated with collagen (Invitrogen). Cells were fixed in ice-cold methanol (Sigma-Aldrich) and then washed and incubated in PBS (Sigma-Aldrich) containing 1% of bovine serum albumin (Sigma-Aldrich) and 0.2% Triton X-100 overnight at 4°C with the appropriate primary and secondary antibodies. The following primary antibodies were used: monoclonal anti-βIII tubulin (Promega; 1:600), polyclonal anti-βIII tubulin (Sigma-Aldrich;1:200), and monoclonal anti-Aβ (1–17) clone 6E10 (Sigma-Aldrich).

For morphological evaluation, slices were mounted and examined by a ZEISS LSM 510 META confocal laser scanning microscope (Carl Zeiss). Images were processed using the LSM5 image examiner (Zeiss). The percentage of morphologically differentiated cells was determined by counting at least 10 fields for each treatment; cells with neurites ≥50 μm in length were considered differentiated.

Western Blot Analysis

Total cell lysates were prepared by scraping the cells in a lysis buffer (50 mM Tris, pH 7.4, 150 mM NaCl, 5 mM EDTA, 1 mM PMSF, 1 mM sodium orthovanadate, 0.5% sodium deoxycholate, 0.5% NP40 with a cocktail of protease inhibitors). For Western blot analysis, 15 μg of total proteins were electrophoresed onto 12% SDS–PAGE and transferred to a nitrocellulose paper. Filters were incubated with anti-Notch1 antibody (Sigma-Aldrich) and with anti-GAPDH (Chemicon, 1:400) as a loading control. An HRP-conjugated antimouse secondary antibody (Dako; 1:1500) and a chemiluminescence blotting substrate kit (Amersham Biosciences) were used for immunodetection. Evaluation of immunoreactivity was performed on immunoblots by densitometric analysis using the Quantity One analysis software (BioRad Laboratories GmbH).

Quantitative Real-Time PCR

Quantitative real-time PCR (QRT-PCR) was executed as described previously (Ferrari-Toninelli et al.[13]). Briefly, the total RNA was isolated from SH-SY5Y and IMR-32 neuroblastoma cells using the RNeasy kit (Qiagen) and digested with the RNase-Free DNAse set (Qiagen), according to the manufacturer's protocol. One microgram of total RNA was transcribed into complementary DNA (cDNA) using murine leukemia virus reverse transcriptase (Promega Italia) and oligodT15-18 as a primer (final volume: 50 μL).

The oligonucleotide sequences of the primers used are as follows: N-Myc forward primer 5′-CGA CCA CAA GGC CCT CAG TA-3′, reverse primer 5′-CAG CCT TGG TGT TGG AGG AG-3′;[38] Hes1 forward primer 5′-CTCTCTTCCCTCCGGACTCT-3′, reverse primer 5′-AGGCGCAATCCAATATGAAC-3′; GAPDH forward primer 5′-AAC TTT GGC ATT GTG GAA GG-3′, reverse primer 5′-ACA CAT TGG GGG TAG GAA CA-3′.

Amplification and detection were performed with the iCYCLER iQ Real-Time PCR Detection System (BioRad Italia); the fluorescence signal was generated by SYBR Green I. Samples were run in triplicate in a 25-μL reaction mix containing 12.5 μL of 2× SYBR Green Master Mix (BioRad Italia), 12.5 pmol of each forward and reverse primer, and 2 μL of diluted cDNA. The PCR program was initiated by 10 minutes at 95°C before 40 cycles, each for 15 seconds at 95°C and 1 minute at 60°C. Gene expression levels were normalized to GAPDH expression, and data are presented as the fold change in target gene expression in drug-treated cells normalized to the internal control gene (GAPDH) and relative to untreated cells. Results were estimated as C_t values; the C_t was calculated as the mean of the C_t for the target gene minus the mean of the C_t for the internal control gene. The C_t represented the mean difference between the C_t of untreated cells minus that of the treated cells. The *N*-fold differential expression in the target gene of drug-treated cells compared with untreated cells was expressed as $2^{-\Delta\Delta C_t}$. Data analysis and graphics were performed using GraphPad Prism 4 software and were the results of a single experiment run in triplicate.

Wound Scratch Assay

Cell migration was analyzed using a modified wound scratch assay; briefly, cells were plated on a dish with a

culture-insert chamber provided with 2-cell culture reservoirs separated by a 400-μm thick wall (IBIDI GmbH), then treated with 10 μM CpdE, 10 μM DAPT, and 1 μM 13-*cis* RA alone or in combination for 5 days, changing the culture medium at day 3. After treatments, chambers were removed and cells were allowed to migrate. Images were taken by a ZEISS LSM 510 META confocal laser scanning microscope (Carl Zeis) immediately after removing the chambers and after 24 hours. This time interval has been chosen because it is shorter than the SH-SY5Y doubling time. Images were processed using the LSM5 image examiner (Zeiss). Four different fields from each sample were considered for quantitative estimation of the distance between the borderlines, and in each image, 8 different equidistant points were measured in order to better estimate the real width of the wounded area. The migration rate is expressed as the percentage of the control. Four independent series of experiments were performed.

Statistical Analysis

Statistical analyses were performed by 1-way analysis of variance followed by Bonferroni's multiple comparison test as post hoc analysis. Data are presented as the mean ± SE. A probability of $<.05$ was considered a significant difference.

Results

Notch Activation Induces Neuroblastoma Cell Growth and Proliferation

The first aim of the study was to establish the contribution of the Notch pathway on neuroblastoma cell growth and proliferation. SH-SY5Y cells were treated with a soluble synthetic form of the Notch ligand Jagged1 (J1), known to induce NICD formation. A 17 amino acid peptide (CDDYYYGFGCNKFCRPR) was synthesized, corresponding to the active sequence of the Jagged1 ligand.[37] A scrambled peptide (RCGPD CFDNYGRYKYCF) was used as a negative control in each experiment (data not shown).

The J1 peptide was added to the culture medium for 24–48 hours, and then the Notch pathway activation was evaluated through the analysis of NICD and Hes1 expression levels. The results in Fig. 1A showed an increase in the NICD levels after 48 hours of J1 exposure. At the same time, Hes1 mRNA levels increased more than 3-fold (Fig. 1B). As shown by immunofluorescence in Fig. 1C, J1-induced Notch activation resulted in significant cell growth; the results of the cell count, shown in Fig. 1D, confirmed a dose-dependent increase in the cell number, reaching its maximum effect with 40 μM J1 peptide (control: 109.6 ± 12.9; J1 20 μM: 142.6 ± 6.3; J1 40 μM: 213 ± 15). In order to assess the proliferation state of SH-SY5Y cells after J1 treatment, Ki-67 positive cells were then counted and revealed a 2-fold increase in proliferating cells (control: 65.3 ± 2.1; J1 40 μM: 124.6 ± 4.2).

*GSIs Cooperate with 13-*cis *RA to Arrest Proliferation of Neuroblastoma Cells*

The effects of GSIs, alone or in combination with 13-*cis* RA, were investigated in SH-SY5Y and IMR-32 cells. CpdE and DAPT were chosen among the different GSIs as potent inhibitors of the Notch signaling pathway. To evaluate the treatments' effect on cell growth and viability, both the cell lines were treated with 10 μM CpdE or 10 μM DAPT alone, with 1 μM 13-*cis* RA alone, or with the combination of all these compounds for 5 days. Cell number and viability were determined at days 1, 3, and 5. The results in Fig. 2 showed both CpdE and DAPT, used as single agents, were able to reduce the cell number in SH-SY5Y and IMR-32 cells. GSIs were more efficacious in *MYCN*-amplified IMR-32 cells, where a complete growth arrest was reached on the first day. The combination of GSIs and 13-*cis* RA resulted in an enhanced growth inhibition resulting in an evident cell loss, with a cell number reduction of about 70%–80% in SH-SY5Y and 90% in IMR-32 cells.

To better investigate these effects, cell cycle analysis was performed on IMR-32 cells treated for 5 days both with the GSIs alone and with the 13-*cis* RA and GSIs combination. The results are shown in Fig. 3A. No significant differences were found in G0/G1, G2/M, or S cell cycle phases in cells treated with GSIs alone, GSIs + 13-*cis* RA, or 13-*cis* RA alone. However, both GSIs used as single compounds and GSIs in combination with 13-cisRA induced an increase in the subG1 phase, suggesting an apoptotic effect of the compounds. The percentages of apoptotic cells (sub G1) were 0.12 ± 0.1, 1.98 ± 0.2, 1.75 ± 0.6, 4.46 ± 0.2, 7.8 ± 0.6, and 11.0 ± 0.6 for DMSO, DAPT, CpdE, 13-*cis* RA, DAPT + 13-*cis* RA, and CpdE + 13-*cis* RA treated cells, respectively.

We further investigated whether GSI treatment induced apoptosis in neuroblastoma cells, by the flow cytometric analysis of Annexin V-positive cells (Fig. 3B and C). The results showed an increase in Annexin V-positive cells after the GSIs treatments, both alone and in combination. In particular, the CpdE treatment induced a significant increase in positive cell percentage compared with the 13-*cis* RA alone. The increase in Annexin V-positive cells after the treatments is a well-recognized biochemical feature of apoptosis in neuroblastoma cells.

*GSIs and 13-*cis *RA Cooperate to Induce Differentiation of Neuroblastoma Cells*

To evaluate the effects of GSIs alone or in combination with 13-*cis* RA in inducing neuroblastoma cell differentiation, SH-SY5Y and IMR-32 cells were exposed for 5 days to 10 μM CpdE or 10 μM DAPT alone, with 1 μM 13-*cis* RA alone, or with the combination of all

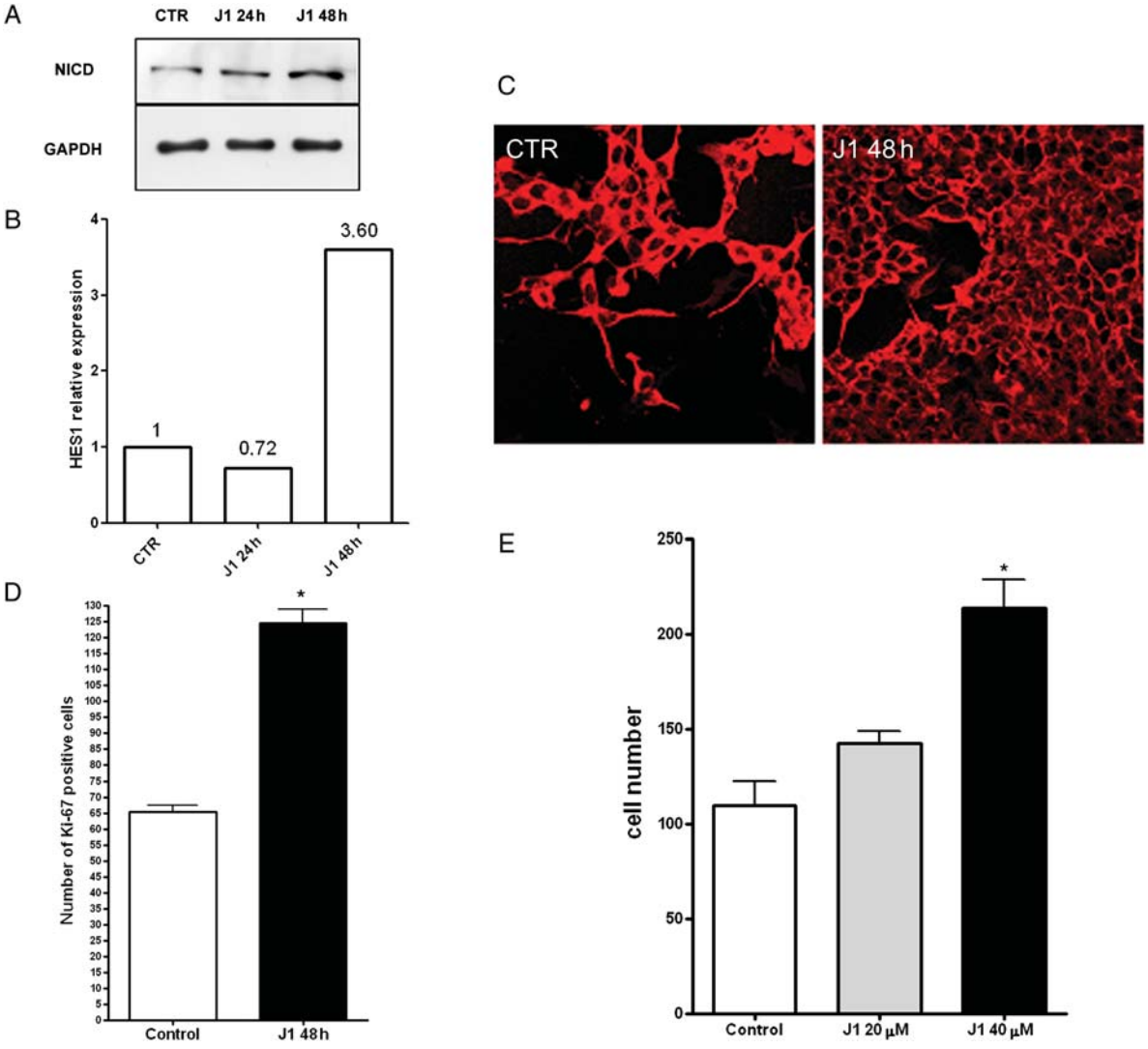

Fig. 1. Jagged1 ligand action on SH-SY5Y neuroblastoma cell growth. (A) Western blot analysis of NICD protein expression levels after 24 and 48 hours of Jagged1 peptide (J1) treatment. GAPDH was used as a loading control. (B) QRT-PCR analysis of HES1 mRNA expression levels after 24 and 48 hours of J1 treatment. (C) Immunofluorescence of SH-SY5Y cells grown for 48 hours in culture medium alone (CTR) or in medium added with 40 μM J1 peptide; βIII tubulin antibody was used to indentify neuroblastoma cells. (D) Cell number determination of SH-SY5Y treated with an increasing dose of J1 for 48 hours. (E) Determination of Ki-67 positive cells in SH-SY5Y neuroblastoma cells untreated or treated for 48 hours with J1 synthetic peptide. *$P < .001$ vs control.

these compounds. At day 5, the morphologic differentiation was evaluated by immunofluorescence after staining with βIII tubulin antibody in order to visualize cell morphology and identify the neurites. As shown in Fig. 4, SH-SY5Y cells treated with GSIs underwent an initial differentiation process characterized by neurite outgrowth in a small number of cells. GSI-induced differentiation was less effective than that obtained using 13-*cis* RA. When GSIs were used in combination with the retinoid, the morphologic differentiation became marked, characterized by the presence of rounded cell bodies and longer neurites with a higher degree of branching and varicosities (arrows). Comparable morphologic results were obtained in IMR-32 cells (data not shown).

A quantitative analysis of morphological differentiation was obtained by measuring neurite length, and the percentage of differentiated cells (defined as cells with neurites ≥ 50 μm in length) was determined (Fig. 5). In both SH-SY5Y and IMR-32 cell lines, GSIs as single agents induced an increase in the number of differentiated cells, although lower than the levels obtained with the differentiating agent 13-*cis* RA. The effect resulted in significant improvement when CpdE and DAPT were combined with RA; in SH-SY5Y cells, both the compounds were shown to enhance the effect when combined with 13-*cis* RA, increasing the percentage of differentiated cells by 2-fold (CpdE + 13-*cis* RA 44.4% ± 4.3% and DAPT + 13-*cis* RA 60.6% ± 10%) compared with 13-*cis* RA alone (27.5% ±

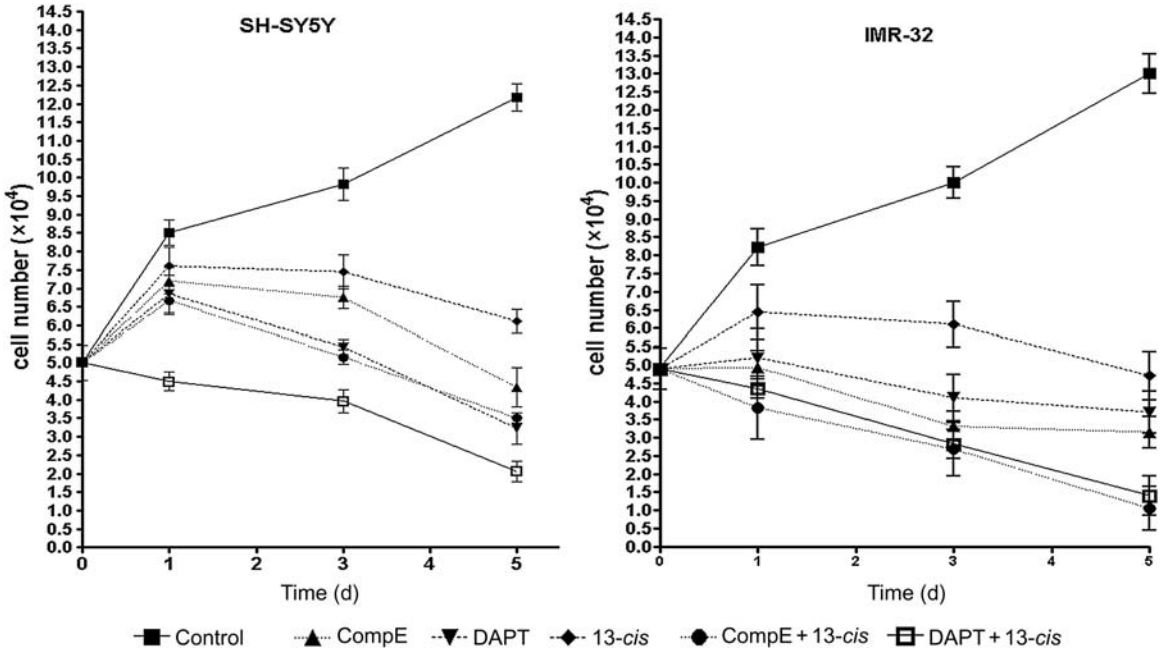

Fig. 2. Quantification of neuroblastoma cell growth induced by GSIs, 13-*cis* RA, or GSIs + 13-*cis* RA. SH-SY5Y and IMR-32 neuroblastoma cells underwent 5 days treatment with GSIs alone or in combination with 13-*cis* RA, and then cell growth was determined by Trypan blue exclusion at days 1, 3, and 5. Data are representative of at least 3 experiments, and values are expressed as the mean ± SE.

3.3%). IMR-32 cells were reported to be resistant to retinoic differentiation due to their amplified MYCN gene,[38] and in this study, 13-*cis* RA treatment exerts a lower effect in IMR-32 cells if compared with SH-SY5Y (8.6% vs 27.5%); however, also in IMR-32 cells, the neurite length was affected by the combined treatments increasing by 2-fold the percentage of differentiated cells (CpdE + 13-*cis* RA, 16.3% ± 2.4; and DAPT + 13-*cis* RA, 15.8% ± 2.3) with respect to 13-*cis* RA alone (8.6% ± 1.6). In summary, GSIs improved the 13-*cis* RA action on neuroblastoma cell differentiation, although the combination does not reach a synergistic effect.

CpdE and DAPT are known as potent inhibitors of Notch cleavage and activation; however, these compounds cannot be considered specific for this signaling pathway, due to their property to cleave several other protein complexes, including the APP.[39] To investigate whether the effects of DAPT and CpdE on neuroblastoma cell proliferation and differentiation was specifically associated with Notch inhibition, neuroblastoma cells were treated with a GSI that does not interfere with the Notch pathway. To this aim, SH-SY5Y cells stably transfected with wt APP[40] were treated for 5 days with the GSI JLK6[41,42] and then analyzed for cell growth and differentiation. As shown in Fig. 6A, JLK6 used at 1 μM (dose devoid of toxic effects in our cellular model) was able to decrease the APP cleavage and Aβ peptide production. In the same experimental setting, JLK6 alone or in combination with 13-*cis* RA was unable to affect cell differentiation (Fig. 6B). Interestingly, treatment of the cells with JLK6 in combination with 13-*cis* RA resulted in significant cell growth arrest (Fig. 6C).

GSIs Revert Cell Migration Induced by 13-cis RA

To study cell motility, we used a modified scratch wound-healing assay. Cells were grown onto a cell culture dish separated by a septum then treated with GSI and 13-*cis* RA, alone or in combination. After 5 days, the septum was removed and the migration extent was measured for each treatment. RA was reported to favor cell migration in SH-SY5Y neuroblastoma cells but not in IMR-32, probably due to the different expression levels of RA receptors.[43,44] Results obtained in the present study showed that, in SH-SY5Y, 13-*cis* RA induced a cell migration increase of about 50%. The contemporary administration of CpdE was found to partially counteract this phenomenon, taking back the cells to the basal migration rate. DAPT, on the contrary, was unable to revertse the RA-induced cell migration.

GSIs alone also significantly reduced the SH-SY5Y migration rate. In particular, CpdE and DAPT treatment caused a 50% and 30% reduction, respectively, of cell motility (Fig. 7).

*N-Myc Expression in Response to GSIs, 13-*cis *RA, and GSIs + 13-cis RA Combined Treatment*

Since the high level of MYCN gene expression is likely to contribute to tumorigenesis and may influence the capacity of differentiation and cell growth inhibition, it was of interest to examine the expression of N-Myc mRNA in response to the different treatments. For this experiment set, SH-SY5Y was used as a cell line without MYCN amplification and IMR-32 and KELLY were chosen as MYCN-amplified cells. Relative N-Myc mRNA levels were confirmed in

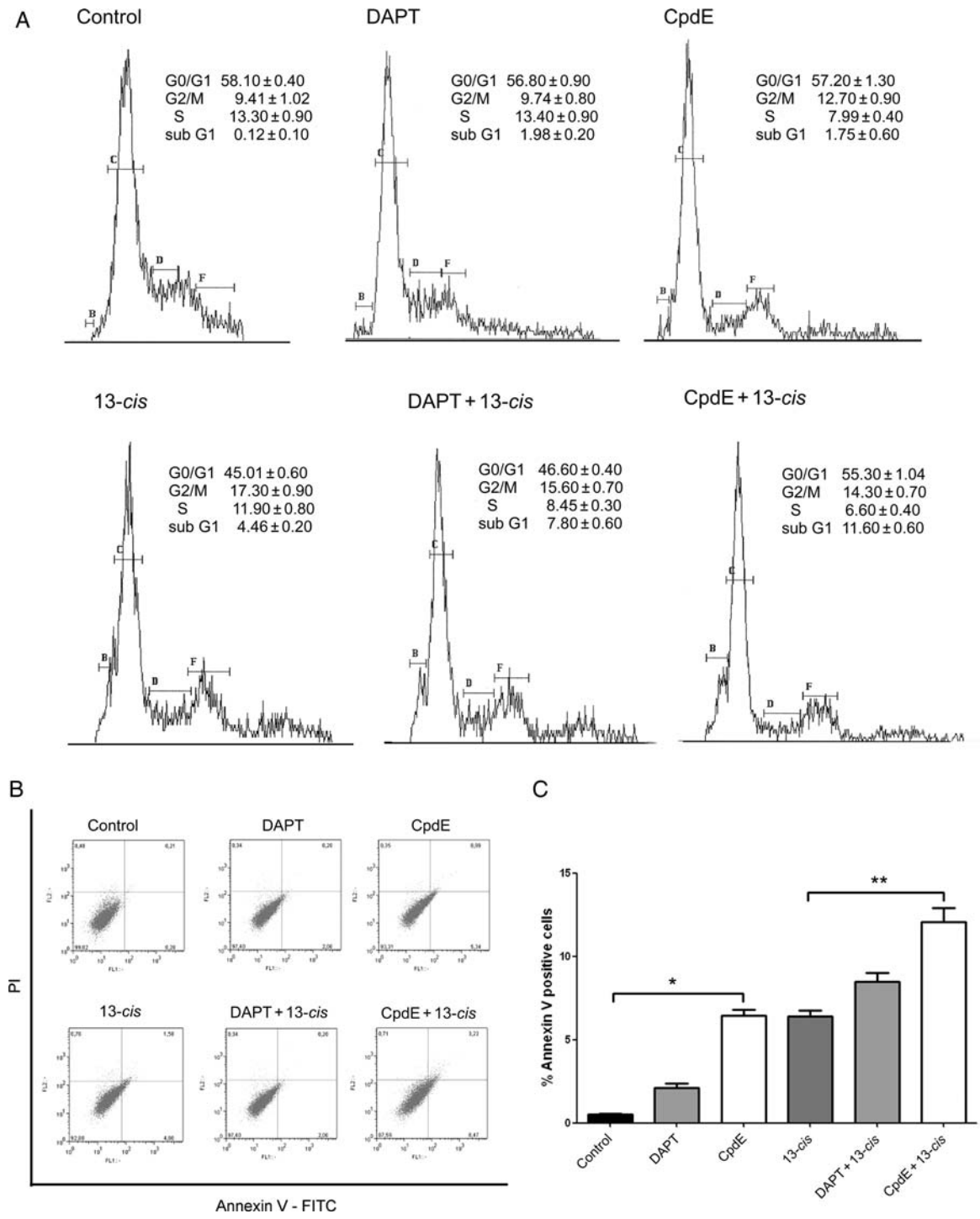

Fig. 3. Cell cycle and apoptosis analysis of neuroblastoma cells after GSIs and 13-*cis* RA treatments. (A) Cell cycle analysis of IMR-32 neuroblastoma cells after 5 days treatment with GSIs alone, 13-*cis* RA, and the GSIs + 13-*cis* RA combination. (B and C) Determination of apoptosis after 3 days treatment with the above-mentioned compounds. (B) Annexin V/PI double staining and flow cytometry assays. *x*-axis indicates the numbers of Annexin V-FITC-stained cells. *y*-axis indicates the number of PI-stained cells. (C) Determination of apoptosis percentages based on the accumulation of Annexin V-positive cells in the A4 area. $*P < .001$ vs control; $**P < .001$ vs 13-*cis* RA.

SH-SY5Y, KELLY, and IMR-32 cell lines by real-time PCR, which revealed very high N-Myc levels in KELLY and IMR-32 cells. In contrast, N-Myc transcripts were barely detectable in SH-SY5Y cells (with a ratio of 1:29 for SH-SY5Y vs KELLY and 1:73 for SH-SY5Y vs IMR-32; Supplementary Material, Fig. S1).

KELLY and IMR-32 cells were exposed for 5 days with GSIs and 13-*cis* RA alone or in combination, and

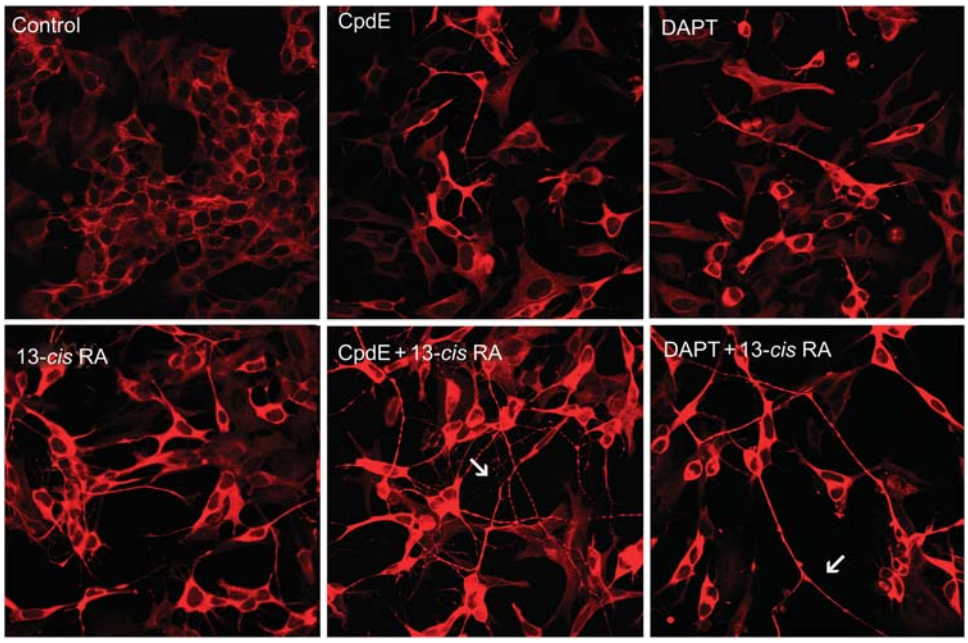

Fig. 4. Neuroblastoma cell differentiation induced by GSIs, 13-*cis* RA, or GSIs + 13-*cis* RA. SH-SY5Y and IMR-32 neuroblastoma cells underwent 5 days treatment with GSIs alone or in combination with 13-*cis* RA, and then neuronal differentiation was evaluated by immunofluorescence and morphometric analysis. Immunofluorescence of SH-SY5Y cells using a βIII tubulin antibody revealed the cell morphology; arrows indicate neurite branching and varicosities.

then the total RNA was extracted and subjected to real-time PCR analysis. In both the cell lines, GSIs and 13-*cis* RA treatments were not able to significantly modify the N-Myc mRNA levels.

Discussion

Innovative therapeutic approaches are strongly needed to counteract the poor prognosis of high-risk neuroblastomas, and the identification of new molecular pathways regulating the tumor progression could open new perspectives in this direction.

In the present study, Notch has been proposed as a potential pathway involved in neuroblastoma pathogenesis. First, a correlation between Notch pathway activation and neuroblastoma cell proliferation was established. Notch activation, which is induced by the Jagged1 ligand, was shown to significantly increase the cell number and proliferation rate, as revealed by the Ki-67 proliferation marker; this observation prompted us to evaluate Notch inhibitors as good candidates to prevent neuroblastoma progression.

Two different GSIs, CpdE and DAPT, were tested in vitro, using as assessment parameters, the cell growth arrest, cytodifferentiation, and cell motility. Both compounds were studied on 2 neuroblastoma cell lines, IMR-32 and SH-SY5Y, respectively, with and without MYCN gene amplification, as a paradigm of 2 different malignancy degrees. These 2 cell lines showed in fact great differences in their proliferation rates, response to differentiating agents, and invasiveness potential, resulting in IMR-32 as high-proliferating and more aggressive cells.[45]

Given that advanced neuroblastoma is often resistant to RA differentiative therapy, all the above parameters were also evaluated for the combination of GSI with 13-*cis* RA.

GSIs as single agents were potent inhibitors of cell growth, and their effects were higher than those obtained with 13-*cis* RA alone; in fact GSIs, also used as single agents, completely arrested cell growth since the first day of treatment in IMR-32 cells. The combination of GSI and 13-*cis* RA led to growth arrest and significant cell loss. GSIs are known to induce cell cycle exit[46] and apoptosis;[47] thus, part of this effect could be attributed to decreased viability. Accordingly, we have found an increase in the subG1 population in the cell cycle analysis and in the number of Annexin V-positive cells after the treatment with the GSIs both alone and in combination with 13-*cis* RA.

In neuroblastoma cell differentiation, GSIs alone showed a low efficacy; however, GSIs were found to enhance the differentiation induced by 13-*cis* RA, suggesting that these compounds act cooperatively to improve the neurite length. Interestingly, in IMR-32 cells, which are known to be resistant to RA differentiation, the neurite length was also affected by the combined treatments, increasing by 2-fold the percentage of the differentiated cells with respect to 13-*cis* RA alone.

These data indicate that the Notch pathway prevents neuronal cell differentiation and suggest that Notch activation could interfere with the activation of 13-*cis* RA action. Notch is indeed known to inhibit neurite

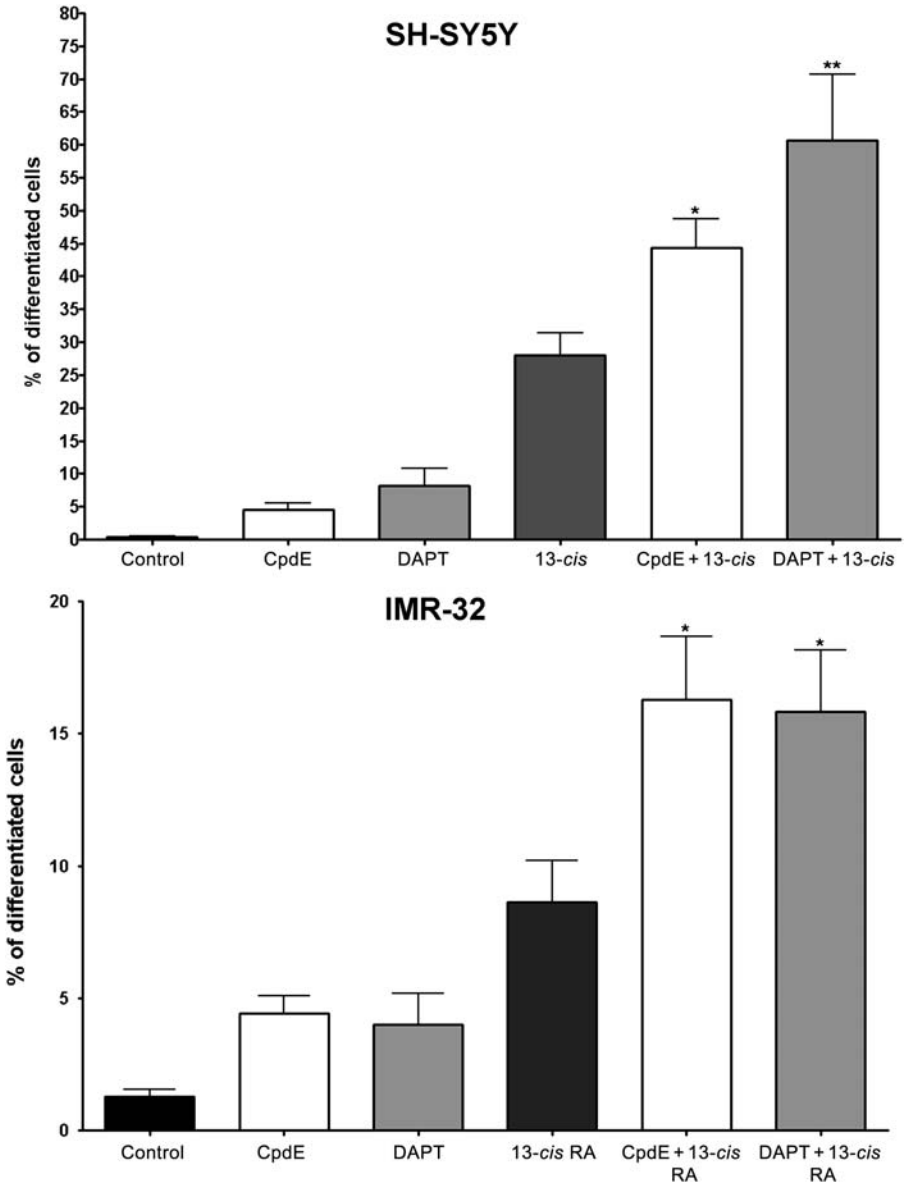

Fig. 5. Morphometric analysis of cell differentiation induced by GSIs, 13-*cis* RA, or GSIs+13-*cis* RA. SH-SY5Y and IMR-32 neuroblastoma cells underwent treatment for 5 days treatment with GSI alone or in combination with 13-*cis* RA, and then neuronal differentiation was evaluated by measuring neurite length. The percentage of differentiated cells was calculated, considered as cells with neurites ≥50 μM in length, in SH-SY5Y and IMR-32 cells. Data are representative of at least 5 experiments. $*P < .05$; $**P < .001$ vs 13-*cis* RA.

outgrowth,[48] and the opposite effect was observed using GSIs;[49] furthermore, SH-SY5Y overexpressing the Notch protein is resistant to RA-induced differentiation.[30] It is tempting to speculate that blocking Notch activation by GSI could reverse the resistance to RA in neuroblastoma. This hypothesis is supported by the observation that GSIs are able to increase chemotherapy sensitivity[50] and to eliminate resistance to glucocorticoids in leukemia.[51]

The Notch pathway was found to participate in many aspects of metastasis, from the epithelial to mesenchymal transition to cell migration and invasion[52] and angiogenesis,[18] and GSIs were shown to reduce cell migration in different cancer cell lines.[16] Here, we showed that GSIs are able to significantly reduce cell migration in SH-SY5Y neuroblastoma cells; furthermore, CpdE counteracts the motility increase induced by 13-*cis* RA in SH-SY5Y cells.

Although further studies are necessary to fully characterize the antimetastatic activity of GSIs, the inhibitory effect of these compounds on neuroblastoma cell migration is of particular interest, given the association between metastatic disease and poor prognosis in this cancer.[53]

The MYCN proto-oncogene plays an important role in neuroblastoma development; about 30%–40% of tumors in an advanced stage exhibit MYCN amplification, which has been related to rapid tumor progression,

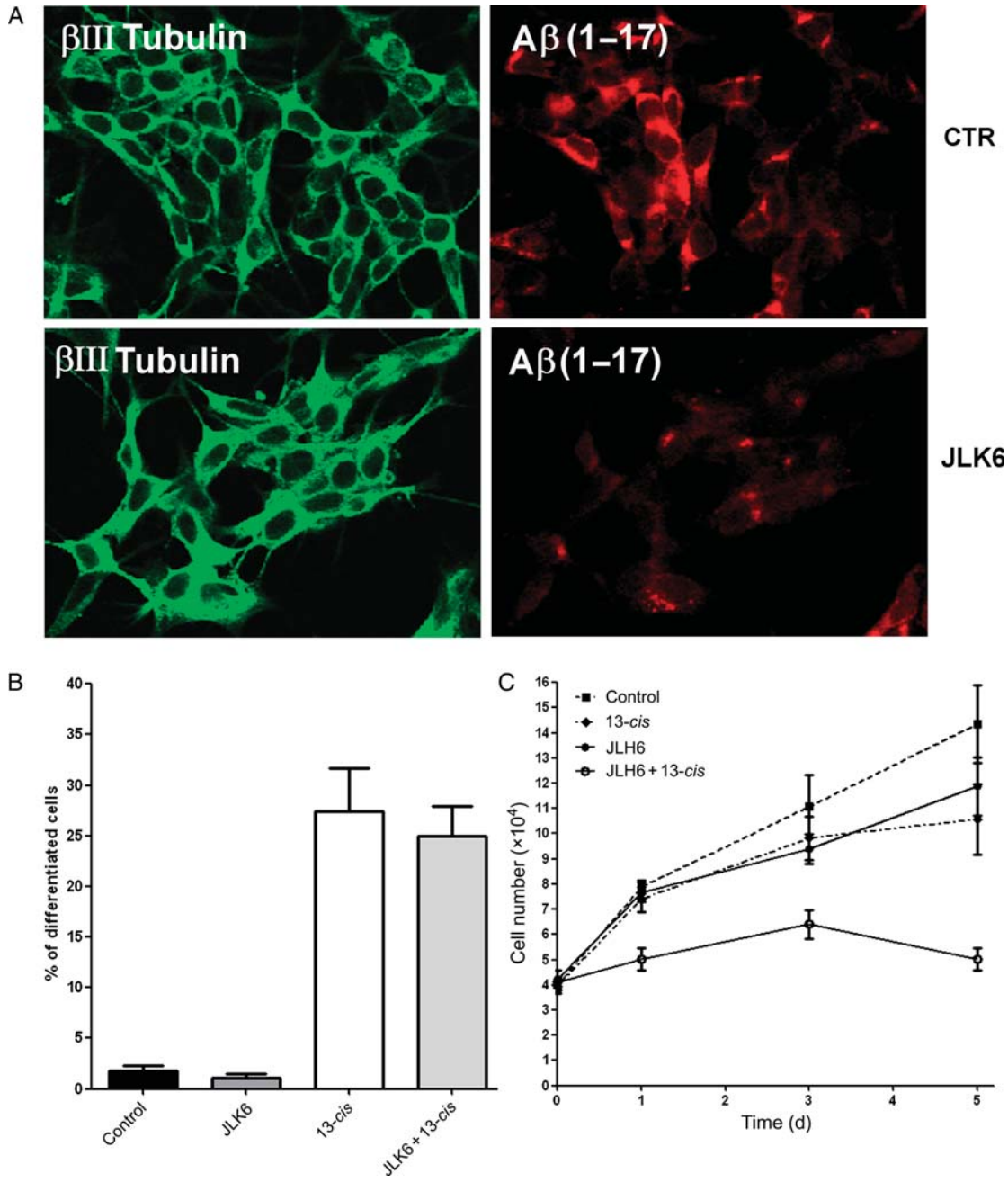

Fig. 6. Neuroblastoma cell proliferation and differentiation analysis after JLK6 treatment. SH-SY5Y neuroblastoma cells stably transfected with APP 751 wild type (SH-SY5Y-APPwt) were treated for 5 days with 1 μM JLK6 GSI, with 1 μM 13-*cis* RA, and with the combination of the 2 compounds. (A) Determination of Aβ peptide levels in control and JLK6-treated cells. The βIII tubulin antibody (green) identified neuronal cells. Anti-Aβ 6E10 antibody (red) was used to detect amino acids 1–17 of Aβ peptide. (B) The Histogram represents the percentage of differentiated cells. (C) Cell growth determination by a Trypan blue exclusion test at 1, 3, and 5 days after treatment.

drug resistance, and poor outcome.[33] MYCN silencing resulted in growth inhibition, apoptosis, and neuroblastoma cell differentiation.[54] In this study, despite evident signs of differentiation and growth arrest, no significant changes in N-Myc mRNA expression occurred in response to GSI, 13 *cis*-RA, or the combination of these drugs. This apparent discrepancy can be explained by the recent demonstration that N-Myc acts upstream of the Notch pathway and activates Notch signaling by inducing the expression of the Notch ligand DLL3.[34] However, the maintenance of high N-Myc mRNA levels also after GSIs and 13-*cis* RA treatment is not incompatible with the growth arrest and differentiation of IMR-32 cells; in fact, other differentiating treatments were found to only slightly affect N-Myc expression.[6] Furthermore, a study of Edsjö et al.[55] demonstrated that N-Myc-amplified neuroblastoma cells retain their capacity to differentiate.

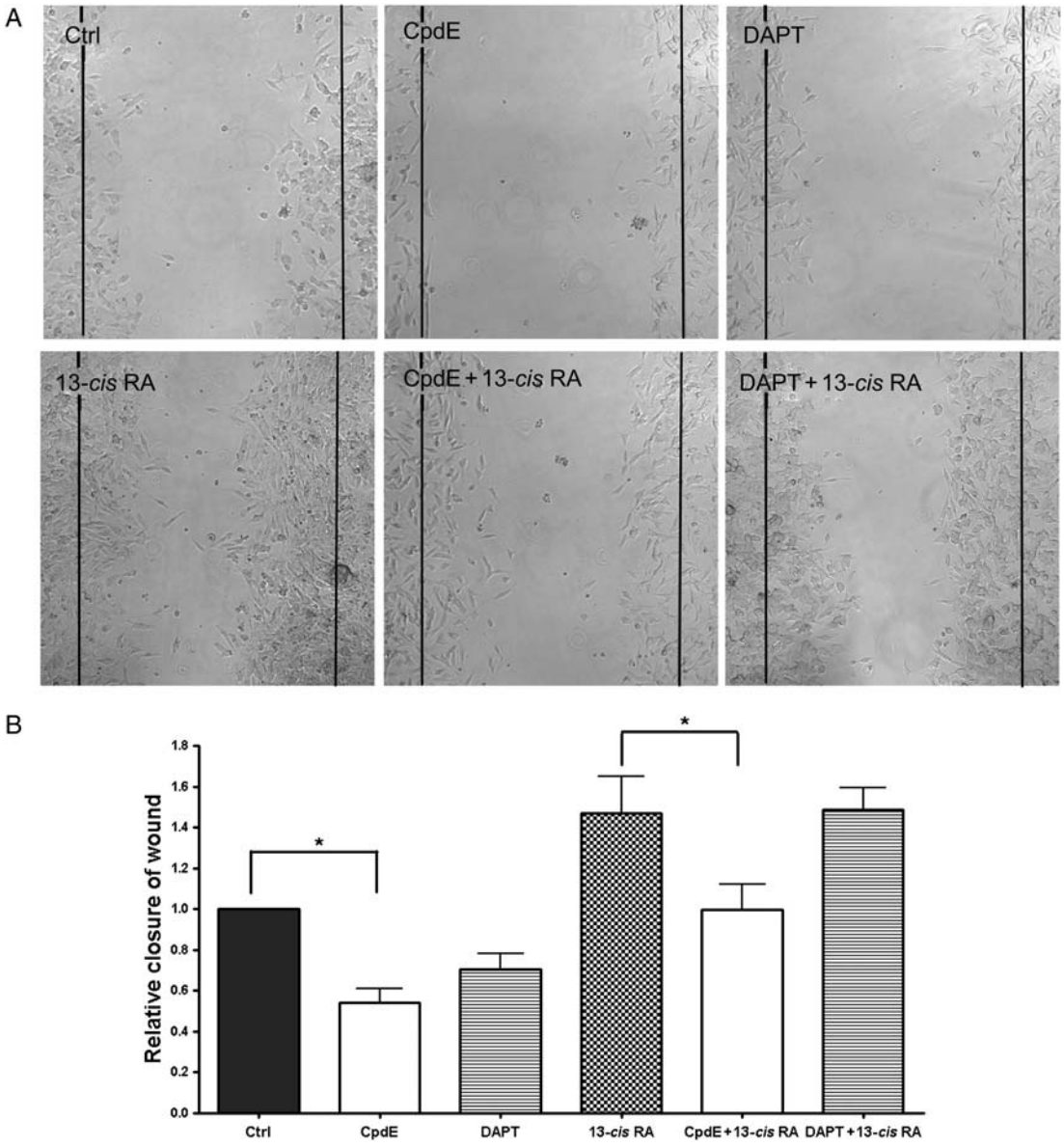

Fig. 7. GSIs inhibit cell motility and revert 13-*cis* RA-induced migration. (A) SH-SY5Y neuroblastoma cells were treated with DMSO (Ctrl) or different drugs as indicated for 5 days and then allowed to migrate for 24 hours after septum removal. Images were taken at time 0 and at 24 hours. (B) Average number of migrated cells from (A). $*P < .05$.

On the whole, our study shows that, as expected, RA exerts a major effect on differentiation and a minor effect on proliferation;[4] on the other hand, GSIs, possibly given to their proapoptotic potential, proved to be more efficacious in inducing growth arrest and cell loss. However, the effects obtained using the 2 agents in combination are always improved and may result in addition or synergy.

Differences were found between CpdE and DAPT depending on the parameters considered. In SH-SY5Y, DAPT resulted in more potent cell growth arrest and differentiation; CpdE is significantly more efficacious in reducing cell motility. Although CpdE is known to be a more potent GSI than DAPT, at the 10-μM concentration used in this study, no differences were detectable between the 2 compounds in blocking Notch cleavage and transcriptional activation.[56] However, about 50 proteins were found as γ-secretase substrates, among which were proteins involved in cancer progression such as p75 neurotrophin and cadherins.[39] Thus, the different efficacy of the 2 compounds could be attributed to the cleavage-blocking activity of selected substrates. In this regard, it should be noted that JLK6, a GSI lacking Notch-blocking activity, was unable to affect neuroblastoma cell differentiation suggesting that at least this specific cell response is under the control of the Notch pathway.

We conclude that GSIs have a pleiotropic effect on neuroblastoma cell lines, including cell growth arrest, induction of differentiation, and cell motility reduction;

furthermore, the combination of GSIs with 13-*cis* RA improves all these effects and may offer a therapeutic advantage for neuroblastoma treatment.

Supplementary Material

Supplementary material is available at *Neuro-Oncology* online.

Acknowledgments

The authors wish to thank Dott. Moris Cadei and Prof. Pier Giovanni Grigolato (2nd Department of Pathology, Spedali Civili and University of Brescia, Italy) for their contribution to the cell cycle analysis.

Conflict of interest statement. None declared.

Funding

This work was supported by the contribution of grants from the Ministry of University and Research (MIUR, Grant #2005051707 to M.M.).

References

1. Maris JM, Hogarty MD, Bagatell R, Cohn SL. Neuroblastoma. *Lancet*. 2007;369(9579):2106–2120.
2. Lau L, Tai D, Weitzman S, Grant R, Baruchel S, Malkin D. Factors influencing survival in children with recurrent neuroblastoma. *J Pediatr Hematol Oncol*. 26:227–232.
3. Matthay KK, Villablanca JC, Seeger RCS, et al. Treatment of high-risk neuroblastoma with intensive chemotherapy, radiotherapy, autologous bone marrow transplantation, and 13-*cis*-retinoic acid. Children's Cancer Group. *N Engl J Med*. 1999;341(16):1165–1173.
4. Garattini E, Gianni' M, Terao M. Cytodifferentiation by retinoids, a novel therapeutic option in oncology: rational combinations with other therapeutic agents. *Vitam Horm*. 2007;75:301–354.
5. De los Santos M, Zambrano A, Aranda A. Combined effects of retinoic acid and histone deacetylase inhibitors on human neuroblastoma SH-SY5Y cells. *Mol Cancer Ther*. 2007;6(4):1425–1432.
6. Guzhova I, Hultquist A, Cetinkaya C, Nilsson K, Påhlman S, Larsson LG. Interferon-gamma cooperates with retinoic acid and phorbol ester to induce differentiation and growth inhibition of human neuroblastoma cells. *Int J Cancer*. 2001;94(1):97–108.
7. Hahn CK, Ross KN, Warrington IM, et al. Expression-based screening identifies the combination of histone deacetylase inhibitors and retinoids for neuroblastoma differentiation. *Proc Natl Acad Sci USA*. 2008;105(28):9751–9756.
8. Brodeur GM. Neuroblastoma: biological insights into a clinical enigma. *Nat Rev Cancer*. 2003;3(3):203–216.
9. Wagner LM, Danks MK. New therapeutic targets for the treatment of high-risk neuroblastoma. *J Cell Biochem*. 2009;107:46–57.
10. Bray SJ. Notch signalling: a simple pathway becomes complex. *Nat Rev Mol Cell Biol*. 2006;7(9):678–689.
11. Louvi A, Artavanis-Tsakonas S. Notch signalling in vertebrate neural development. *Nat Rev Neurosci*. 2006;7(2):93–100.
12. Sestan N, Artavanis-Tsakonas S, Rakic P. Contact-dependent inhibition of cortical neurite growth mediated by Notch signaling. *Science*. 1999;286(5440):741–746.
13. Ferrari-Toninelli G, Bonini SA, Bettinsoli P, Uberti D, Memo M. Microtubule stabilizing effect of Notch activation in primary cortical neurons. *Neuroscience*. 2008;154(3):946–952.
14. Ferrari-Toninelli G, Bonini SA, Uberti D, et al. Notch activation induces neurite remodeling and functional modifications in SH-SY5Y neuronal cells. *Dev Neurobiol*. 2009;69(6):378–391.
15. Leong KG, Karsan A. Recent insights into the role of Notch signaling in tumorigenesis. *Blood*. 2006;107(6):2223–2233.
16. Sâhlgren C, Gustafsson MV, Jin S, Poellinger L, Lendahl U. Notch signalling mediates hypoxia-induced tumor cell migration and invasion. *Proc Natl Acad Sci USA*. 2008;105(17):6392–6397.
17. Rehman AO, Wang CY. Notch signaling in the regulation of tumor angiogenesis. *Trends Cell Biol*. 2006;16(6):293–300.
18. Dufraine J, Funahashi Y, Kitajewski J. Notch signaling regulates tumor angiogenesis by diverse mechanisms. *Oncogene*. 2008;27(38):5132–5137.
19. Bolós V, Blanco M, Medina V, Aparicio G, Díaz-Prado S, Grande E. Notch signalling in cancer stem cells. *Clin Transl Oncol*. 2009;11(1):11–19.
20. Miele L, Miao H, Nickoloff BJ. Notch signaling as a novel cancer therapeutic target. *Curr Cancer Drug Targets*. 2006;6(4):313–323.
21. Rizzo P, Osipo C, Foreman K, Golde T, Osborne B, Miele L. Rational targeting of Notch signaling in cancer. *Oncogene*. 2008;27(38):5124–5131.
22. De Keersmaecker K, Lahortiga I, Mentens N, et al. In vitro validation of gamma secretase inhibitors alone or in combination with other anti-cancer drugs for treatment of T-cell acute lymphoblastic leukaemia. *Haematologica*. 2008;93(4):533–542.
23. Baliko F, Bright T, Poon R, Cohen B, Egan SE, Alman BA. Inhibition of Notch signaling induces neural differentiation in Ewing sarcoma. *Am J Pathol*. 2007;170(5):1686–1694.
24. Hallahan AR, Pritchard JI, Hansen S, et al. The SmoA1 mouse model reveals that Notch signaling is critical for the growth and survival of sonic hedgehog-induced medulloblastoma. *Cancer Res*. 2004;64(21):7794–7800.
25. Shih IeM, Wang TL. Notch signaling, gamma-secretase inhibitors, and cancer therapy. *Cancer Res*. 2007;67(5):1879–1882.
26. Påhlman S, Stockhausen MT, Fredlund E, Axelson H. Notch signaling in neuroblastoma. *Semin Cancer Biol*. 2004;14:365–373.
27. Sarovina K, Schellenberger J, Schneider C, et al. Progenitor cell maintenance and neurogenesis in sympathetic ganglia involves Notch signalling. *Mol Cell Neurosci*. 2008;37:20–31.
28. Revet I, Huizenga G, Chan A, et al. The MSX1 homeobox transcription factor is a downstream target of PHOX2B and activates the Delta-Notch pathway in neuroblastoma. *Exp Cell Res*. 2008;314(4):707–719.
29. Grynfeld A, Påhlman S, Axelson H. Induced neuroblastoma cell differentiation, associated with transient HES-1 activity and reduced HASH-1 expression, is inhibited by Notch1. *Int J Cancer*. 2000;88:401–410.

30. Hooper C, Tavassoli M, Chapple PJ, et al. TAp73 isoforms antagonize Notch signalling in SH-SY5Y neuroblastomas and in primary neurones. *J Neurochem*. 2006;99:989–999.
31. Stockhausen MT, Sjölund J, Axelson H. Regulation of the Notch target gene Hes-1 by TGFα induced Ras/MAPK signalling in human neuroblastoma cells. *Exp Cell Res*. 2005;310:218–228.
32. Kim Y, Lin Q, Zelterman D, et al. Hypoxia regulated Delta-like 1 homologue enhance cancer cell stemness and tumorigenicity. *Cancer Res*. 2009;69(24):9271–9280.
33. Pession A, Tonelli R. The MYCN oncogene as a specific and selective drug target for peripheral and central nervous system tumors. *Curr Cancer Drug Targets*. 2005;5(4):273–283.
34. Zhao X, D' Arca D, Lim WK, et al. The N-Myc-DLL3 cascade is suppressed by the ubiquitin ligase Huwe1 to inhibit proliferation and promote neurogenesis in the developing brain. *Dev Cell*. 2009;17(2):210–221.
35. Janardhanan R, Banik NL, Ray SK. N-Myc down regulation induced differentiation, early cell cycle exit, and apoptosis in human malignant neuroblastoma cells having wild type or mutant p53. *Biochem Pharmacol*. 2009;78:1105–1114.
36. Funahashi Y, Hernandez SL, Das I, et al. A Notch1 ectodomain construct inhibits endothelial Notch signaling, tumor growth, and angiogenesis. *Cancer Res*. 2008;68(12):4727–4735.
37. Nickoloff BJ, Quin JZ, Chaturvedi V, Denning MF, Bonish B, Miele L. Jagged-1 mediated activation of Notch signalling induces complete maturation of human keratinocytes through NF-κB and PPARγ. *Cell Death Diff*. 2002;9:842–855.
38. Bordow SB, Haber M, Madafiglio J, Cheung B, Marshall GM, Norris MD. Expression of the multidrug resistance-associated protein (MRP) gene correlates with amplification and overexpression of the N-myc oncogene in childhood neuroblastoma. *Cancer Res*. 1994;54(19):5036–5040.
39. Lleò A. Activity of γ-secretase on substrate other than APP. *Curr Top Med Chem*. 2008;8:9–16.
40. Zampagni M, Evangelisti E, Cascella R, et al. Lipid rafts are primary mediators of amyloid oxidative attack on plasma membrane. *J Mol Med*. 2010;88(6):597–608.
41. Petit A, Pasini A, Alves da Costa C, et al. JLK isocoumarin inhibitors: selective g-secretase inhibitors that do not interfere with Notch pathway in vitro or in vivo. *J Neurosci Res*. 2003;74:370–377.
42. Hellström M, Phng LK, Hofmann JJ, et al. Dll4 signalling through Notch1 regulates formation of tip cells during angiogenesis. *Nature*. 2007;445(7129):776–780.
43. Joshi S, Guleria RS, Pan J, Dipette D, Singh US. Heterogeneity in retinoic acid signaling in neuroblastomas: Role of matrix metalloproteinases in retinoic acid-induced differentiation. *Biochim Biophys Acta*. 2007; 1772(9):1093–1102.
44. Joshi S, Guleria R, Pan J, DiPette D, Singh US. Retinoic acid receptors and tissue-transglutaminase mediate short-term effect of retinoic acid on migration and invasion of neuroblastoma SH-SY5Y cells. *Oncogene*. 2006;25(2):240–247.
45. Zaizen Y, Taniguchi S, Suita S. The role of cellular motility in the invasion of human neuroblastoma cells with or without N-myc amplification and expression. *J Pediatr Surg*. 1998;33(12):1765–1770.
46. Rao SS, O'Neil J, Liberator CD, et al. Inhibition of NOTCH signaling by gamma secretase inhibitor engages the RB pathway and elicits cell cycle exit in T-cell acute lymphoblastic leukaemia cells. *Cancer Res*. 2009;69(7):3060–3068.
47. Rasul S, Balasubramanian R, Filipović A, Slade MJ, Yagüe E, Coombes RC. Inhibition of gamma-secretase induces G2/M arrest and triggers apoptosis in breast cancer cells. *Br J Cancer*. 2009;100(12): 1879–1888.
48. Berezovska O, McLean P, Knowles R, et al. Notch1 inhibits neurite outgrowth in postmitotic primary neurons. *Neuroscience*. 1999;93(2): 433–439.
49. Liao YF, Wang BJ, Hsu WM, et al. Unnatural substituted (hydroxyethyl urea) peptidomimetics inhibit gamma secretase and promote the neuronal differentiation of neuroblastoma cells. *Mol Pharmacol*. 2007;71(2):588–601.
50. Nefedova Y, Sullivan DM, Bolick SC, Dalton WS, Gabrilovich DI. Inhibition of Notch signaling induces apoptosis of myeloma cells and enhances sensitivity chemotherapy. *Blood*. 2008;111(4):2220–2229.
51. Real PJ, Tosello V, Palomero T, Castillo M, et al. Gamma-secretase inhibitors reverse glucocorticoid resistance in T cell acute lymphoblastic leukemia. *Nat Med*. 2009;15(1):50–58.
52. Bailey JM, Singh PK, Hollingsworth MA. Cancer metastasis facilitated by developmental pathways: Sonic hedgehog, Notch, and bone morphogenic proteins. *J Cell Biochem*. 2007;102(4):829–839.
53. Garaventa A, Perilongo G. High risk neuroblastoma: a persistent therapeutic challenge. *Pediatr Blood Cancer*. 2008;51:722–723.
54. Nara K, Kusafuka T, Yoneda A, Oue T, Sangkhathat S, Fukuzawa M. Silencing of MYCN by RNA interference induces growth inhibition, apoptotic activity and cell differentiation in a neuroblastoma cell line with MYCN amplification. *Int J Oncol*. 2007;30(5):1189–1196.
55. Edsjö A, Nilsson H, Vandesompele J, Karlsson J, Pattyn F, Culp LA, et al. Neuroblastoma cells with overexpressed MYCN retain their capacity to undergo neuronal differentiation. *Lab Invest*. 2004;84(4): 406–417.
56. Yang T, Arslanova D, Gu Y, Augelli-Szafran C, Xia W. Quantification of gamma-secretase modulation differentiates inhibitor compound selectivity between two substrates Notch and amyloid precursor protein. *Mol Brain*. 2008;1(1):15.